

Stochastic Deep-Ritz for Parametric Uncertainty Quantification

Ting Wang^a, Jaroslaw Knap^a

^a *Physical Modeling and Simulation Branch, DEVCOM Army Research Laboratory, Aberdeen Proving Ground, MD, 21005-5066, USA*

Abstract

Scientific machine learning has become an increasingly popular tool for solving high dimensional differential equations and constructing surrogates of complex physical models. In this work, we propose a deep learning based numerical method for solving elliptic partial differential equations (PDE) with random coefficients. We elucidate the stochastic variational formulation for the problem by recourse to the direct method of calculus of variations. The formulation allows us to reformulate the random coefficient PDE into a stochastic optimization problem, subsequently solved by a combination of Monte Carlo sampling and deep-learning approximation. The resulting method is simple yet powerful. We carry out numerical experiments to demonstrate the efficiency and accuracy of the proposed method.

Keywords: Deep learning, random coefficient PDE, uncertainty quantification, Monte Carlo, scientific machine learning

1. Introduction

Randomness and uncertainty are ubiquitous in science and engineering. In order to facilitate reliable decision making with known levels of confidence, it is often essential to quantify the uncertainty in physical systems. A good case in point is additive manufacturing of materials. Additive manufacturing usually involves numerous sources of uncertainty such as laser power, material composition or particle size. The uncertainty ultimately influences the material microstructure and hence, in turn, affects the mechanical performance of manufactured parts. Therefore, it is critical to take the uncertainty into account as to clear the way for robust additive manufacturing. From the mathematical modeling perspective, the uncertainty is frequently modeled as the random input data in the form of a random field κ to a differential equation

$$\mathcal{L}_\kappa(u)(x) = f(x) \quad \text{in } D. \quad (1)$$

Here, \mathcal{L}_κ is a differential operator over the domain D dependent on a random field κ , f is the forcing and the solution u is the quantity of interest.

A great number of computational methodologies have been developed to solve random coefficient PDEs of type (1). Among them, stochastic collocation (SC), stochastic Galerkin (SG), and Monte Carlo (MC)/quasi Monte Carlo (QMC) are the three mainstream approaches. SC aims to first solve the deterministic counterpart of (1) on a set

of collocation points and then interpolate over the entire image space of the random element [1, 2, 3]. Hence, the method is non-intrusive, meaning that it can take advantage of existing solvers developed for deterministic problems. Similarly, MC is non-intrusive since it relies on taking sample average over a set of deterministic solutions computed from a set of realizations of the random field [4, 5, 6]. In contrast, SG is considered as intrusive since it requires a construction of discretization of both the stochastic space and physical space simultaneously and, as a result, it commonly tends to produce large systems of algebraic equations whose solutions are needed [4, 7, 8, 9, 10]. However, these algebraic systems differ appreciably from their deterministic counterparts and thus existing deterministic solvers can rarely be utilized.

We emphasize that all traditional methods suffer from the curse of dimensionality and hence tend to be limited to low dimensional problems (e.g., $D \subset \mathbb{R}^2$ or $D \subset \mathbb{R}^3$). Recently, deep neural networks (DNN) have garnered some acceptance in computational science and engineering, and deep-learning-based computational methods have been universally recognized as potentially capable of overcoming the curse of dimensionality [11, 12]. Depending on how the loss function is formulated, deep-learning-based methods for deterministic PDEs can broadly be classified into three categories: 1) residual based minimization, 2) deep backward stochastic differential equations (BSDE) and 3) energy based minimization. Both the physics informed neural networks (PINNs) [13, 14] and the deep Galerkin methods (DGMs) [15] belong to the category of residual minimization. PINNs aim to minimize the total residual loss based on a set of discrete data points in the domain D . Similarly, DGMs rely on minimizing the loss function induced by the L^2 error. We also refer [16, 17] for a similar approach. In contrast, the deep-BSDE methods exploit the intrinsic connection between PDEs and BSDEs in the form of the nonlinear Feynman-Kac formula to recast a PDE as a stochastic control problem that is solved by reinforcement learning techniques [18, 19, 20, 21, 22]. See [23] for a recent work on interpolating between PINNs and deep BSDEs. Finally, energy methods construct the loss function by taking advantage of the variational formulation of elliptic PDEs [24, 25, 26, 27]. As a comparable approach, in [28] the Dynkin formula for overdamped Langevin dynamics is employed to construct a weighted variational loss function. We refer an interested reader to [29, 30, 31] for an in-depth overview of deep-learning-based methods for solving PDEs.

Recently, extensions of the deep-learning approaches for PDEs with random coefficients have been proposed. For example, convolutional neural networks mimicking image-to-image regression in computer vision have been employed to learn the input-to-output mapping for parametric PDEs [26, 32, 33]. However, these methods, by design, are mesh-dependent and therefore aim to discover a mapping between finite dimensional spaces. In comparison, operator learning methods, such as the operator network (ONet) [34] and the Fourier neural operator (FNO) [35], attempt to learn a mesh-free, infinite dimensional operator with deep learning. Let us point out that all these methods tend to identify a mapping $u : \kappa \rightarrow u(\kappa)$, i.e., from the random field to the solution. In practice, the sampling of κ often taken reliant on the Karhunen–Loève expansion to parameterize κ by means of a finite dimensional random vector Z . Taking this fact into account, in this work we propose to directly learn a mapping $u : (x, Z) \rightarrow u(x, Z)$, i.e., from the joint space of x and Z to the solution. This formulation bypasses the difficulty of designing special network architectures for operator learning and hence the problem can be solved with fully connected neural network architectures. Moreover, ONet and FNO are supervised by design and rely on the mean square loss function to facilitate training.

Such a loss function rarely takes (1) into account in a direct manner and customarily depends on sampling of the solution throughout the domain. In order to sidestep the above difficulties, we instead employ the variational formulation whose Euler-Lagrange equations yield (1). More specifically, we focus on the following variational problem

$$\min_u \mathbb{E} \left[\int_D I_\omega(x, u, \nabla u) dx \right] \quad (2)$$

for a function I_ω depending on the random element ω . We emphasize that our approach possesses a fundamental advantage over the approaches reliant on (1). Namely, after approximating the solution u by a DNN, the functional provides a natural loss function. Hence, the physical laws encoded in (2) are seamlessly incorporated when a minimizer is computed. Our method can be considered as an extension of the deep-Ritz method in [24] to the stochastic setting and henceforth we refer to it as the stochastic deep-Ritz method.

The remainder of the article is organized as follows. Section 2 describes the problem setup and provides the theoretical foundations for the stochastic variational formulation of the problem. In Section 3, we propose the DNN based approach and present the stochastic deep-Ritz method. Finally, numerical benchmarks are presented in Section 4.

2. The stochastic variational formulation

2.1. Problem setup

Let $D \subset \mathbb{R}^d$ be a bounded open set with a Lipschitz boundary and $(\Omega, \mathcal{F}, \mathbb{P})$ be a probability space, where Ω is the sample space, $\mathcal{F} \subset 2^\Omega$ is a σ -algebra of all possible events and $\mathbb{P} : \mathcal{F} \rightarrow [0, 1]$ is a probability measure. We consider the following random coefficient linear elliptic equation defined on $(\Omega, \mathcal{F}, \mathbb{P})$: for almost all $\omega \in \Omega$,

$$\begin{aligned} -\nabla \cdot (\kappa(x, \omega) \nabla u(x, \omega)) &= f(x, \omega) && \text{in } D, \\ u(x, \omega) &= 0 && \text{on } \partial D, \end{aligned} \quad (3)$$

where the diffusion coefficient $\kappa : D \times \Omega \rightarrow \mathbb{R}$ is a random field with continuous and bounded covariance functions. We underscore that the methodology developed here generalizes to semilinear problems with nonhomogenous Dirichlet or Neumann boundary conditions [36]. However, for the ease of presentation, we restrict the discussion to the form of (3).

Under the usual assumption that the random fields can be completely parameterized by a finite dimensional random vector $Z = (Z_1, \dots, Z_K) : \Omega \rightarrow \Gamma \subset \mathbb{R}^K$, i.e., there exists finitely many uncorrelated random variables Z_1, \dots, Z_K such that

$$\kappa(x, \omega) = \kappa(x, Z(\omega)), \quad f(x, \omega) = f(x, Z(\omega)),$$

problem (3) becomes

$$\begin{aligned} -\nabla \cdot (\kappa(x, Z(\omega)) \nabla u(x, Z(\omega))) &= f(x, Z(\omega)), && \text{in } D, \\ u(x, Z(\omega)) &= 0, && \text{on } \partial D. \end{aligned} \quad (4)$$

Let us stress that we do not require the set Γ to be uniformly bounded, which is often assumed for the SC method.

We draw attention of the reader to the fact that in our approach we do not seek solutions of problem (4) as we employ it simply to motivate subsequent developments. Instead, we focus entirely on a more fundamental concept from which problem (4) originates: the minimization of a stochastic functional. The benefits of such an approach are twofold. First, minimizers of the stochastic functional generally form a broader class of functions than solutions of problem (4). Given the flexibility of DNN when it comes to function interpolation, this broader class can be potentially explored. More importantly, however, the stochastic functional constitutes a natural loss function and no ansatz pertaining to a form of the loss function is needed. Hence, our method adheres strictly to the underlying model of a physical phenomena.

2.2. Function space and the stochastic weak form

We now set up an appropriate function space for the problem. We introduce the physical space $H_0^1(D)$, i.e., the Sobolev space of functions with weak derivatives up to order 1 and vanishing on the boundary. To define the function space for Z , we assume that Z admits a probability density function $\rho(z)$ so that

$$\mathbb{E}[g(Z(\omega))] = \int_{\Gamma} g(z)\rho(z) dz$$

for any measurable function $g : \Gamma \rightarrow \mathbb{R}$. Then we define the stochastic space $L_\rho^2(\Gamma)$, i.e.,

$$L_\rho^2(\Gamma) = \left\{ g : \Gamma \rightarrow \mathbb{R} \mid \int_{\Gamma} |g(z)|^2 \rho(z) dz = \mathbb{E}[|g(Z)|^2] \right\},$$

which is the ρ -weighted L^2 space. The solution $u(x, Z)$ to (4) is thus defined in the space

$$L^2(\Gamma, H_0^1(D)) = \left\{ v : D \times \Gamma \rightarrow \mathbb{R} \mid v \text{ is strongly measurable and } \|v\|_{H_0^1(D)} \in L_\rho^2(\Gamma) \right\}, \quad (5)$$

where the norm $\|\cdot\|_{L^2(\Gamma, H_0^1(D))}$ is induced by the inner product:

$$\begin{aligned} \langle u, v \rangle &= \int_{\Gamma} \int_D u(x, z)v(x, z)\rho(z) dx dz + \int_{\Gamma} \int_D \nabla u(x, z) \cdot \nabla v(x, z)\rho(z) dx dz \\ &= \mathbb{E} \left[\int_D u(x, Z)v(x, Z) dx \right] + \mathbb{E} \left[\int_D \nabla u(x, Z) \cdot \nabla v(x, Z) dx \right]. \end{aligned} \quad (6)$$

Under certain conditions, a direct application of the Lax-Milgram theorem immediately implies the well-posedness of the following stochastic weak form of (4):

$$\mathbb{E} \left[\int_D \kappa(x, Z) \nabla u(x, Z) \cdot \nabla v(x, Z) - f(x, Z)v(x, Z) dx \right] = 0, \quad \forall v \in L^2(\Gamma, H_0^1(D)). \quad (7)$$

The above stochastic weak form is equivalent to a min-max problem which involves a saddle points searching. Therefore, it is possible to solve the problem using deep learning frameworks such as the generative adversarial network (GAN) and its variants [37, 38]. However, it is well known that training of GAN is a difficult task often requiring fine tuning of hyper-parameters. The training becomes even more challenging in the context of PDEs. We refer the reader to [39] for a recent work on solving deterministic PDEs using GAN.

2.3. The stochastic variational form

Owing to the difficulty of training GAN models based on the stochastic weak form, we alternatively reformulate (4) into the following stochastic variational problem

$$\min_{u \in L^2(\Gamma, H_0^1(D))} J(u) \quad \text{with} \quad J(u) = \mathbb{E} \left[\int_D \frac{1}{2} \kappa(x, Z) |\nabla u(x, Z)|^2 - f(x, Z) u(x, Z) dx \right]. \quad (8)$$

This stochastic variational problem can be viewed as an extension of the Ritz formulation (or Dirichlet's principle) to the stochastic setting. The following theorem provides the theoretical justification of the stochastic variational reformulation.

Theorem 2.1. *Under the following two assumptions:*

A1. *The diffusivity coefficient $\kappa(x, Z)$ is uniformly bounded and uniformly coercive, i.e., there exist constants $0 < \kappa_{\min} \leq \kappa_{\max}$ such that for almost all $\omega \in \Omega$,*

$$\mathbb{P}(\omega \in \Omega : \kappa_{\min} \leq \kappa(x, Z(\omega)) \leq \kappa_{\max}, \forall x \in \bar{D}) = 1.$$

A2. *The forcing $f(x, Z)$ satisfies the following integrability condition:*

$$\mathbb{E} \left[\int_D |f(x, Z)|^2 dx \right] < \infty.$$

Then the stochastic optimization problem (8) admits a minimizer $u^ \in L^2(\Gamma, H_0^1(D))$. Furthermore, u^* satisfies the stochastic weak form (7).*

Proof. To show the existence of a minimizer u^* to (8), it is sufficient to show that 1) there exists a minimizing sequence $u_n(x, Z)$ (up to a subsequence) that converges weakly to some $u^* \in L^2(\Gamma, H_0^1(D))$ and 2) the functional $J(u)$ is (weakly) lower semicontinuous [40].

Denote $J^* = \inf\{J(u) \mid u \in L^2(\Gamma, H_0^1(D))\}$. Note that $J^* > -\infty$ and hence there exists a minimizing sequence u_n such that $J(u_n) \rightarrow J^*$. We shall show that there exists $u^* \in L^2(\Gamma, H_0^1(D))$ such that $J^* = J(u^*)$.

For weak convergence of the sequence $u_n(x, Z)$, it suffices to uniformly bound u_n in $L^2(\Gamma, H_0^1(D))$. To this end, note that by the assumption on κ ,

$$\frac{1}{2} \kappa(x, Z) |\nabla u_n(x, Z)|^2 - f(x, Z) u_n(x, Z) \geq \frac{1}{2} \kappa_{\min} |\nabla u_n(x, Z)|^2 - f(x, Z) u_n(x, Z).$$

Integrating over D and taking expectation of both sides lead to

$$J(u_n) \geq \frac{1}{2} \kappa_{\min} \mathbb{E} \left[\int_D |\nabla u_n(x, Z)|^2 dx \right] - \mathbb{E} \left[\int_D f(x, Z) u_n(x, Z) dx \right].$$

Invoking the assumption on κ and the Cauchy-Schwarz inequality leads to

$$J(u_n) \geq C_1 \mathbb{E} \left[\|\nabla u_n(\cdot, Z)\|_{L^2(D)}^2 \right] - \mathbb{E} \left[\|f(\cdot, Z)\|_{L^2(D)}^2 \right]^{\frac{1}{2}} \mathbb{E} \left[\|u_n(\cdot, Z)\|_{L^2(D)}^2 \right]^{\frac{1}{2}},$$

where $C_1 = \kappa_{\min}/2$. By the assumption on f and the Poincaré's inequality, there exists a constant $C_2 > 0$ (which depends on f and the domain D) such that

$$J(u_n) \leq C_1 \mathbb{E} \left[\|\nabla u_n(\cdot, Z)\|_{L^2(D)}^2 \right] - C_2 \mathbb{E} \left[\|\nabla u_n(\cdot, Z)\|_{L^2(D)}^2 \right]^{\frac{1}{2}}.$$

Now note that $J(u_n)$ is uniformly bounded (in n) since it is a minimizing sequence of (8), which implies $\mathbb{E}\{\|\nabla u_n(\cdot, Z)\|_{L^2(D)}^2\}$ is uniformly bounded (in n) and hence

$$\sup_n \mathbb{E}\{\|u_n(\cdot, Z)\|_{H_0^1(D)}^2\} < \infty.$$

Therefore, there exists a subsequence, still denoted by u_n , that converges weakly to some $u^* \in L^2(\Gamma, H_0^1(D))$.

Next, we justify that $J(u)$ is (weakly) lower semicontinuous. For each $z \in \mathbb{R}^K$, define the functional $L_z : D \times \mathbb{R} \times \mathbb{R}^n \rightarrow \mathbb{R}$ by

$$L_z(x, u, \xi) = \frac{1}{2} \kappa(x, z) |\xi|^2 + f(x, z)u.$$

Since $(u, \xi) \mapsto L_z(x, u, \xi)$ is convex for every x and z , we have for all $x \in D$ and almost all $\omega \in \Omega$,

$$\begin{aligned} L_{Z(\omega)}(x, u_n, \nabla u_n) &\geq L_{Z(\omega)}(x, u^*, \nabla u^*) + \partial_u L_{Z(\omega)}(x, u^*, \nabla u^*)(u_n - u^*) \\ &\quad + \partial_\xi L_{Z(\omega)}(x, u^*, \nabla u^*) \cdot (\nabla u_n - \nabla u^*). \end{aligned}$$

Integrating both sides of the above inequality and then taking expectations lead to

$$J(u_n) \geq J(u^*) + \mathbb{E} \left[\int_D f(x, Z)(u_n - u^*) dx \right] + \mathbb{E} \left[\int_D \kappa(x, Z) \nabla u^* \cdot (\nabla u_n - \nabla u^*) dx \right].$$

Since u_n converges weakly to u^* in $L^2(\Gamma, H_0^1(D))$ and both $f(x, Z)$ and $\kappa(x, Z) \nabla u^*$ are in $L^2(\Gamma, H_0^1(D))$, we immediately have

$$\liminf_{n \rightarrow \infty} J(u_n) \geq J(u^*).$$

Therefore, $J(u)$ is (sequentially weak) lower semicontinuous and hence u^* is a minimizer by the direct method of calculus of variation.

It remains to be shown that u^* satisfies the weak form (7). To this end, we consider the functional J evaluated at $u^* + \epsilon v$ for every $v \in L^2(\Gamma, H_0^1(D))$. A simple calculation shows that the Gateaux derivative satisfies

$$\lim_{\epsilon \rightarrow 0} \frac{1}{\epsilon} (J(u^* + \epsilon v) - J(u^*)) = \mathbb{E} \left[\int_D \kappa(x, Z) \nabla u^* \cdot \nabla v - f(x, Z) v dx \right].$$

Since u^* is a minimizer of J , the Gateaux derivative

$$\left. \frac{d}{d\epsilon} \right|_{\epsilon=0} J(u^* + \epsilon v) = 0,$$

and hence the weak form (7). □

In the following section, we present a numerical method for solving the stochastic variational problem (8).

3. Stochastic deep-Ritz: deep learning based UQ

3.1. Preliminaries on neural networks

Let us now briefly review some preliminaries on DNN and set up the finite dimensional functional space induced by DNN. A standard fully-connected DNN of depth $L > 2$ with input dimension N_0 and output dimension N_L is determined by a tuple

$$\Phi = \{(T_1, \sigma_1), \dots, (T_L, \sigma_L)\},$$

where $T_l(x) = W_l x + b_l$ is an affine transformation with weight matrix $W_l \in \mathbb{R}^{N_{l-1} \times N_l}$ and bias vector $b_l \in \mathbb{R}^{N_l}$ and $\sigma_l : \mathbb{R}^{N_l} \rightarrow \mathbb{R}^{N_l}$ is a nonlinear activation function. We say the DNN Φ is of width W if $W = \max_{l=1, \dots, L} N_l$. We denote

$$\theta = (W_1, b_1, \dots, W_L, b_L)$$

the weight parameters of Φ and

$$\sigma = (\sigma_1, \dots, \sigma_L)$$

the set of activation functions of Φ . For a fixed set of activation functions σ , the DNN Φ is completely determined by the weight parameters θ and hence in the sequel we write $\Phi = \Phi_\theta$ to emphasize the dependence on θ . Each DNN Φ_θ induces a function

$$u_\theta = R(\Phi_\theta) : \mathbb{R}^{N_0} \rightarrow \mathbb{R}^{N_L}, \quad x \mapsto \sigma_L \circ T_L \circ \dots \circ \sigma_1 \circ T_1.$$

We refer to $R(\Phi_\theta)$ as the realization of the DNN Φ_θ . The set of all DNNs of depth L and width W , denoted by $\mathcal{N}_{L,W}$, induces a functional space $\mathcal{U}_{L,W}$ consisting of all realizations of DNNs contained in $\mathcal{N}_{L,W}$, i.e.,

$$\mathcal{U}_{L,W} = \{u_\theta : \mathbb{R}^{N_0} \rightarrow \mathbb{R}^{N_L} \mid u_\theta = R(\Phi_\theta), \Phi_\theta \in \mathcal{N}_{L,W}\}.$$

Approximating a function u by DNNs in $\mathcal{N}_{L,W}$ amounts to selecting a realization $u_\theta \in \mathcal{U}_{L,W}$ minimizing a suitable loss functions. Therefore, a DNN along with its realization together provide a surrogate over the finite dimensional space $\mathcal{U}_{L,W}$.

3.2. The stochastic deep-Ritz method

We are now in a position to discuss solving the stochastic optimization problem (8) with DNN. To avoid the deterministic approximation of the integration over the physical domain D , we introduce a random variable X with the uniform density function $\mu(x)$ supported on D and rewrite (8) into the following fully probabilistic form:

$$\min_{u \in L^2(\Gamma, H_0^1(D))} J(u) \quad \text{with} \quad J(u) = \mathbb{E} \left[\frac{1}{2} \kappa(X, Z) |\nabla u(X, Z)|^2 - f(X, Z) u(X, Z) \right], \quad (9)$$

where the expectation \mathbb{E} is taken with respect to both X and Z and we implicitly assume that the volume of D with respect to μ is normalized to 1, i.e., $\int_D \mu(x) dx = 1$.

Next, we seek an approximate solution of the problem (9) in the finite dimensional space $\mathcal{U}_{L,W}$. The functional in (9) provides a natural loss function that can be optimized

with DNN using SGD methods. Specifically, we consider a class of DNNs Φ_θ (parameterized by θ) with input dimension $d + K$ and output dimension 1 whose realizations approximate the true solution $u(x, z)$, i.e.,

$$u(x, z) \approx u_\theta(x, z) = R(\Phi_\theta)(x, z),$$

through minimizing the functional (9). This leads to the following finite dimensional optimization problem:

$$\min_{u_\theta \in \mathcal{U}_{L,W}} J(u_\theta) \quad \text{with} \quad J(u_\theta) = \mathbb{E} \left[\frac{1}{2} \kappa(X, Z) |\nabla u_\theta(X, Z)|^2 - f(X, Z) u_\theta(X, Z) \right],$$

where the optimization is over the space $\mathcal{U}_{L,W}$, i.e., the function space induced by the realizations of DNNs with depth L and width W . The fully-connected DNN architecture that we employ in this work is schematically represented in Figure 1. Although there exist more sophisticated NN architectures, e.g., residual NN [41], we demonstrate in Section 4 that a rather simple fully-connected DNN is capable of learning the solution with high accuracy.

Unlike the finite element method which takes the boundary conditions into account by design, DNN-based methods do not allow to automatically enforce the boundary conditions. Therefore, we introduce a penalty term to compensate for the boundary condition and obtain the final loss function:

$$\min_{u_\theta \in \mathcal{U}_{L,W}} J(u_\theta) \tag{10}$$

with

$$J(u_\theta) = \mathbb{E} \left[\frac{1}{2} \kappa(X, Z) |\nabla u_\theta(X, Z)|^2 - f(X, Z) u_\theta(X, Z) \right] + \beta \mathbb{E} [|u_\theta(S, Z)|^2],$$

where β is the penalty coefficient and S is a random variable with a uniform distribution over the boundary ∂D . Here, the first and second expectations are taken with respect to (X, Z) and (S, Z) , respectively. But we use the same \mathbb{E} to denote the two expectations for notational simplicity. The stochastic optimization problem (10) can be naturally solved by the SGD algorithm or its variants and the final stochastic deep-Ritz algorithm is presented in Algorithm 1.

Remark 3.1. *Some remarks on Algorithm 1 are in order.*

1. *A natural choice for the stochastic gradient estimator is*

$$g(\theta; X, S, Z) = \nabla_\theta \left\{ \frac{1}{2} \kappa(X, Z) |\nabla u_\theta(X, Z)|^2 - f(X, Z) u_\theta(X, Z) + \beta |u_\theta(S, Z)|^2 \right\},$$

which can be easily obtained by automatic differentiation in any deep learning frameworks. However, it is possible to construct more efficient estimators through variance reduction techniques [42, 43]. This will be the focus of another work.

2. *The numerical consistency of the stochastic deep-Ritz method, i.e., the minimizer of $J(u_\theta)$ over $\mathcal{U}_{L,W}$ converges (weakly) to the minimizer of $J(u)$ over $L^2(\Gamma, H_0^1(D))$, relies on justifying the Γ -convergence when either the depth $L \rightarrow \infty$ or the width $W \rightarrow \infty$ (see e.g., [44]). This will be the focus of another theoretical work. We refer interested reader to [27] for a proof in the deterministic setting.*

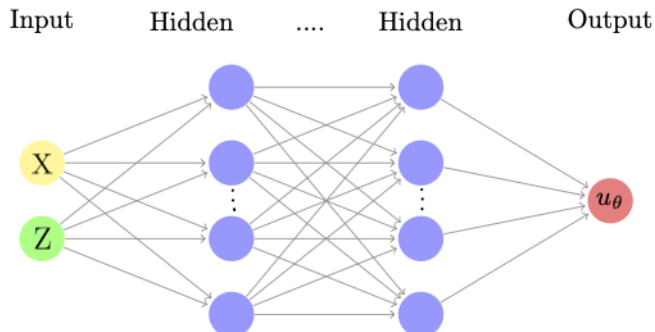


Figure 1: The fully-connected neural network architecture employed in the stochastic deep-Ritz solver.

Algorithm 1 The stochastic deep-Ritz algorithm

Input: A fully-connected DNN Φ_θ ; Number of training epochs N ; Mini-batch size M ; penalty coefficient β ; learning rate η_n ;

Output: A DNN surrogate Φ_θ with realization u_θ .

- 1: **for** $n = 1 : N$ **do**
- 2: Generate a minibatch of samples (X_m, S_m, Z_m) for $m = 1, \dots, M$,
- 3: Evaluate the NN realizations $u_\theta(X_m, Z_m)$ and $u_\theta(S_m, Z_m)$,
- 4: Compute the stochastic gradient estimator $g(\theta_n; X_m, S_m, Z_m)$ such that

$$\mathbb{E}[g(\theta_n; X_m, S_m, Z_m)] = \nabla_\theta J(\theta_n), \quad m = 1, \dots, M,$$

- 5: Compute the mini-batch average:

$$\bar{g}(\theta_n) = \frac{1}{M} \sum_{m=1}^M g(\theta_n; X_m, S_m, Z_m),$$

- 6: Update the DNN parameters: $\theta_n \leftarrow \theta_n - \eta_n \bar{g}(\theta_n)$.
-

3. *In practice, more efficient SGD variants such as Adam can be used to expedite the training of NNs [45].*

It should be emphasized that the stochastic deep-Ritz method learns a deterministic function u_θ mapping the random variables X and Z to the random variable $u_\theta(X, Z)$. Similar applications of DNNs are common in deep learning. For instance, the generator of a GAN learns a mapping from Gaussian samples to samples from the desired distribution. Similarly, the DNN in our method takes samples from (X, Z) and learns how to generate samples from $u_\theta(X, Z)$, that is, the DNN learns the transformation between (X, Z) and $u_\theta(X, Z)$. In comparison with the traditional approaches, e.g., SC and PC, which obtain an explicit approximation to the solution, the proposed methodology should be considered as an implicit method since it only allows us to learn an approximated simulator of the true solution $u(X, Z)$. However, note that for stochastic problems, one is often not interested in the analytical solutions but rather the statistical properties (e.g., moments, distribution) of the solution. In practice, all statistical properties of the solution can be

easily computed through sampling directly from the learned neural DNN.

4. Numerical experiments

In this section, we assess the numerical performance of the stochastic deep-Ritz solver in order to demonstrate the efficiency and accuracy of the algorithm. We measure the accuracy of the DNN realization $u_\theta(x, Z)$ using the relative L^2 mean error

$$E(\theta) = \frac{\mathbb{E}[|u_\theta(X, Z) - u(X, Z)|^2]}{\mathbb{E}[|u(X, Z)|^2]}.$$

For all the numerical examples considered in this section, we use the fully-connected DNN architecture (see Figure 1) with the tanh activation function and apply the Adam optimizer [45] to train the DNN. All numerical experiments are implemented with the deep learning framework PyTorch [46] on a Tesla V100-SXM2-16GB GPU.

4.1. A one-dimensional problem

In the first example, we test the performance of the stochastic deep-Ritz solver by considering the following one-dimensional problem:

$$\begin{aligned} -(\kappa(x, Z)u'(x, Z))' &= 0, & \text{in } D &= [-1, 1] \\ u(-1, Z) &= 0, \\ u(+1, Z) &= 1. \end{aligned} \tag{11}$$

The random field $\kappa(x, Z)$ is taken to be log-normal of the form $\kappa = e^{\beta V(x, Z)}$ with $\beta = 0.1$, where the potential V is a nonlinear function of the random vector $Z = (A_1, \dots, A_n, B_1, \dots, B_n)$, namely,

$$V(x, Z) = \frac{1}{\sqrt{n}} \sum_{k=1}^n A_k \cos(\pi k x) + B_k \sin(\pi k x)$$

and A_k and B_k are independent unit-normal random variables. One can easily verify that $V(x, Z)$ is a Gaussian random field with zero mean and the covariance kernel

$$\text{cov}(x_1, x_2) = \frac{1}{n} \sum_{k=1}^n \cos(\pi k(x_2 - x_1)).$$

It can be shown that the exact solution of the problem (11) is

$$u(x, Z) = \left(\int_{-1}^1 \frac{1}{\kappa(\xi, Z)} d\xi \right)^{-1} \int_{-1}^x \frac{1}{\kappa(\xi, Z)} d\xi$$

We test the algorithm for this problem with $n = 5$. To approximate the solution, we use a fully-connected DNN with $L = 5$ layers, $W = 256$ nodes per layer and tanh activation function. To account for the boundary condition, we set the penalty coefficient to be $\beta = 50$. For the training of the DNN, we run the solver for 4×10^5 epochs with a minibatch size $M = 2560$ per epoch. The initial learning rate is set to $\eta = 10^{-3}$ and

is reduced by a factor of 10 after every 10^5 epochs. At the end of the training, the final relative L^2 mean error is $E(\theta) = 0.52\%$. To further test the accuracy of the learned DNN, we compare the marginal distributions of the learned solution $u_\theta(X, Z)$ and the exact solution $u(X, Z)$ in Figure 2. The results demonstrate that our method approximates the true random field solution fairly accurately.

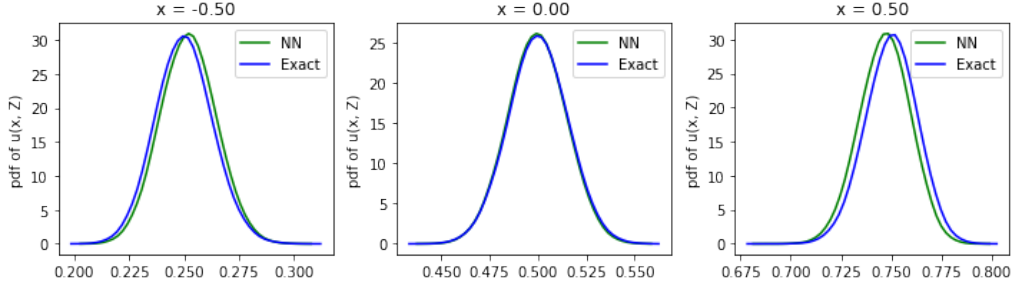


Figure 2: Marginal distributions of the solution to the 1d Dirichlet problem. Left: the pdf of $u_\theta(x, Z)$ at $x = -0.5$; Center: the pdf of $u_\theta(x, Z)$ at $x = 0$; Right: the pdf of $u_\theta(x, Z)$ at $x = 0.5$.

Finally, we visualize the joint density function for $u_\theta(-0.5, Z)$ and $u_\theta(0.5, Z)$ in Figure 3, which verifies that the approximated solution $u_\theta(x, Z)$ captures the correct correlation of the random field at different x .

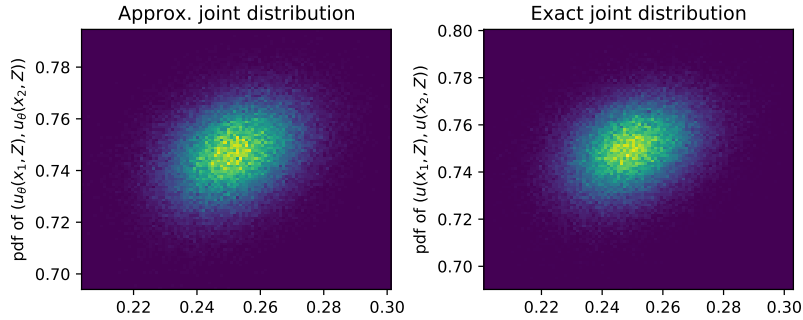


Figure 3: Joint distribution of the solution to the 1d Dirichlet problem. Left: the approximated joint pdf of $u_\theta(-0.5, Z)$ and $u_\theta(0.5, Z)$; Right: the exact joint pdf $u(-0.5, Z)$ and $u(0.5, Z)$.

4.2. A semilinear problem with Neumann boundary condition

Next, we consider a semilinear problem over $D = [0, 1]^d$:

$$-\nabla \cdot (\kappa(x, Z) \nabla u(x, Z)) = f(x, u(x, Z), Z) \quad \text{in } D \quad (12)$$

with the Neumann boundary condition

$$\frac{\partial u}{\partial n}(x, Z) = 0 \quad \text{on } \partial D.$$

The random field κ is here

$$\kappa(x, Z) = d + 1 + \sum_{i=1}^d Z_i$$

with $Z = (Z_1, \dots, Z_d)$ uniformly distributed over D and the semilinear term f is given by

$$f(x, u(x, Z), Z) = -\pi^2(d + 1 + \sum_{i=1}^d Z_i) u(x, Z) + 2\pi^2 \sum_{i=1}^d \cos(\pi x_i).$$

It can be easily verified that the unique solution is

$$u(x, Z) = \frac{1}{\kappa(x, Z)} \sum_{i=1}^d \cos(\pi x_i).$$

To solve the above minimization problem numerically, we approximate the solution $u(X, Z)$ by a DNN realization $u_\theta(X, Z)$ and formulate the following variational problem:

$$\min_{\theta} J(\theta) \quad \text{with} \quad J(\theta) = \mathbb{E} \left[\frac{1}{2} (\kappa(X, Z) |\nabla u_\theta(X, Z)|^2 - f(X, u_\theta(X, Z), Z) u_\theta(X, Z)) \right].$$

Note that this problem does not require a penalty term and hence the ground truth remains unchanged.

In the numerical experiment with $d = 2$, we use a $L = 5$ layer fully-connected DNN with $W = 32$ nodes in each layer and tanh activation. We train the DNN for 3×10^5 epochs with a minibatch size 2560 per epoch. The initial learning rate is set to $\eta = 10^{-4}$ and is decayed by a factor of 0.1 after every 10^5 epochs. We test the accuracy of the trained DNN solution by computing the relative L^2 mean error using a Monte Carlo integration. Based on 10^4 test samples, the final relative L^2 mean error is $E(\theta) = 0.65\%$. The decays of both the loss function $J(\theta)$ and the relative L^2 mean error $E(\theta)$ with respect to the number of training epochs are visualized in Figure 4, which demonstrates a consistent convergence behavior of $J(\theta)$ and $E(\theta)$. These results confirm that minimizing the loss $J(\theta)$ leads to a good approximation to the true solution.

To demonstrate the distributional behavior of the DNN solution $u_\theta(X, Z)$, we compare its distribution to the distribution of the true solution $u(X, Z)$ at various values of X . The probability density functions (PDF) are shown in Figure 5. These results clearly indicate that the stochastic deep-Ritz solver is capable of capturing the distributional property of the true random field.

We conclude this subsection by applying the stochastic deep-Ritz method to the Neumann problem (12) in $d = 10$ dimensions. We employ the same DNN architecture, number of training epochs and minibatch size as that for the case $d = 2$. We set the initial learning rate to $\eta = 10^{-5}$ and decay it after every 10^5 epochs by a factor of 10. The final relative L^2 mean error $E(\theta)$ turns out to be 0.93% and the numerical results for the marginal distributions $u_\theta(\cdot, Z)$ are presented in Figure 6. The results confirm that, with the same computational cost, the stochastic deep-Ritz method maintains the desired accuracy for high dimensional problems, a clear indication that the method may have the potential to overcome the curse of dimensionality.

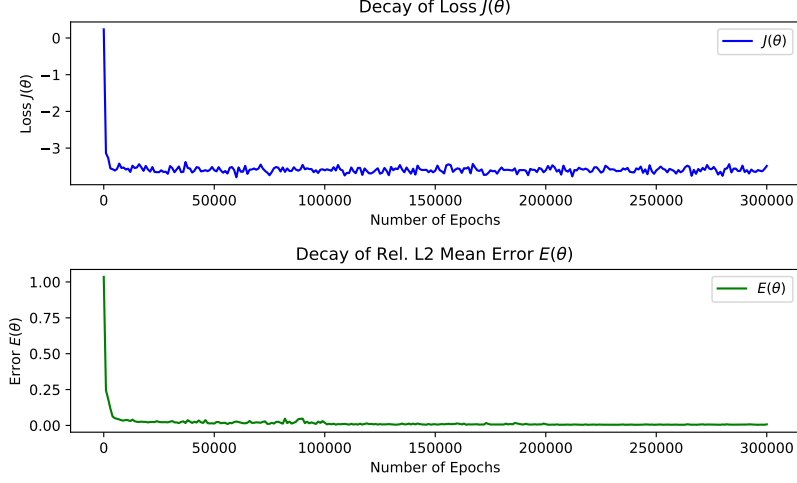


Figure 4: Convergence of the stochastic deep-Ritz applied to the Neumann problem

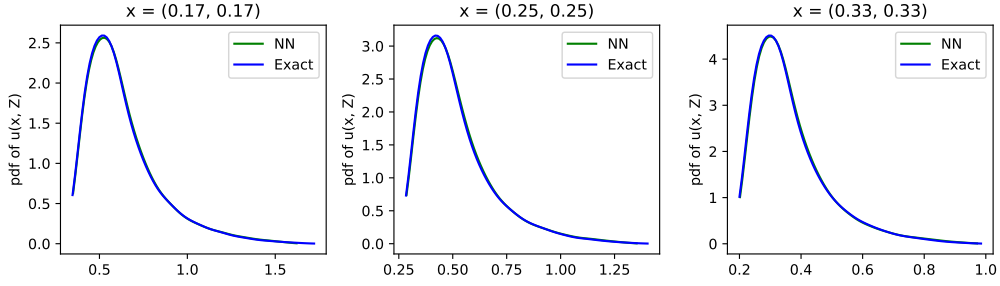


Figure 5: Marginal distributions of the solution to the 2 dimensional Neumann problem. Left: the pdf of $u_\theta(x, Z)$ at $x = (1/6, 1/6)$; Center: the pdf of $u_\theta(x, Z)$ at $x = (1/4, 1/4)$; Right: the pdf of $u_\theta(x, Z)$ at $x = (1/3, 1/3)$.

4.3. A Dirichlet boundary condition

In this numerical example, we apply the proposed stochastic deep-Ritz solver to the following Dirichlet boundary problem:

$$-\nabla \cdot (\kappa(x, Z) \nabla u(x, Z)) = 2\pi^2 \sin(\pi x_1) \sin(\pi x_2), \quad \text{in } D = [-1, 1]^2 \quad (13)$$

with a zero boundary condition $u(x, Z) = 0$ on ∂D . Here, the random field is defined as

$$\kappa(x, Z) = 3 + Z_1 + Z_2$$

with $Z = (Z_1, Z_2)$ follows an uniform distribution over $[-1, 1]^2$. The problem admits the unique solution

$$u(x, Z) = \frac{1}{\kappa(x, Z)} \sin(\pi x_1) \sin(\pi x_2).$$

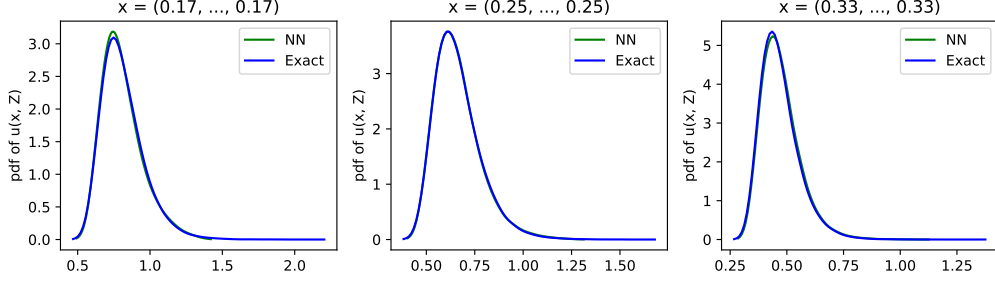


Figure 6: Marginal distributions of the solution to the 10 dimensional Neumann problem. Left: the pdf of $u_\theta(x, Z)$ at $x = (1/6, \dots, 1/6) \in \mathbb{R}^{10}$; Center: the pdf of $u_\theta(x, Z)$ at $x = (1/4, \dots, 1/4) \in \mathbb{R}^{10}$; Right: the pdf of $u_\theta(x, Z)$ at $x = (1/3, \dots, 1/3) \in \mathbb{R}^{10}$.

In order to solve the problem using DNN, we seek for a minimizer of the loss function of the form (10).

The numerical experiment is carried out with a $L = 5$ layer fully-connected DNN with $W = 256$ nodes per layer and the tanh activation function. The DNN is trained for 4×10^5 epochs using 2560 samples per minibatch for each epoch. We use a learning rate scheduling with the initial learning rate $\eta = 10^{-3}$ and decay the learning rate by a factor of 10 after every 10^5 epochs. We plot the loss function $J(\theta)$ and the relative L^2 mean error $E(\theta)$ in Figure 7, which again demonstrates that $J(\theta)$ and $E(\theta)$ decay in a consistent manner. Note that there is a clear decrease of $E(\theta)$ after the first 10^5 epochs due to the learning rate scheduling.

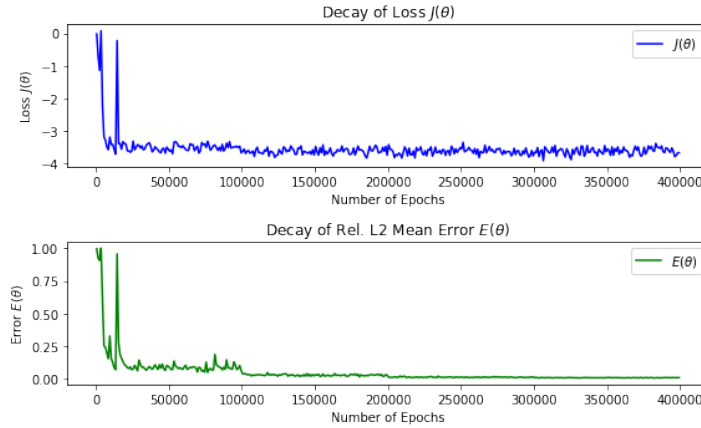


Figure 7: Convergence of the stochastic deep-Ritz applied to the Dirichlet problem. The first 1000 epochs is skipped in the plot.

We gauge the accuracy of the DNN solution $u_\theta(x, Z)$ by comparing it to the exact solution $u(x, Z)$. With 10^5 Monte Carlo test samples, the relative L^2 mean error is $E(\theta) = 0.96\%$. To further assess the accuracy of the approximated solution $u_\theta(x, Z)$, we plot the marginal distribution and the joint distribution of the random field in Figure 8

and Figure 9, respectively. The numerical results suggest that the stochastic deep-Ritz method achieves a highly accurate approximation to the true solution.

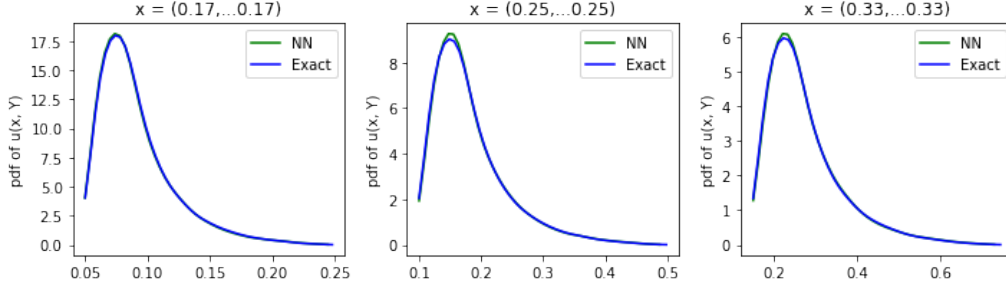


Figure 8: Distributions of the solution to the Dirichlet problem with penalty coefficient $\beta = 500$. Left: the (unnormalized) pdf of $u_\theta(x, Z)$ at $x = (1/6, 1/6)$; Center: the (unnormalized) pdf of $u_\theta(x, Z)$ at $x = (1/4, 1/4)$; Right: the (unnormalized) pdf of $u_\theta(x, Z)$ at $x = (1/3, 1/3)$.

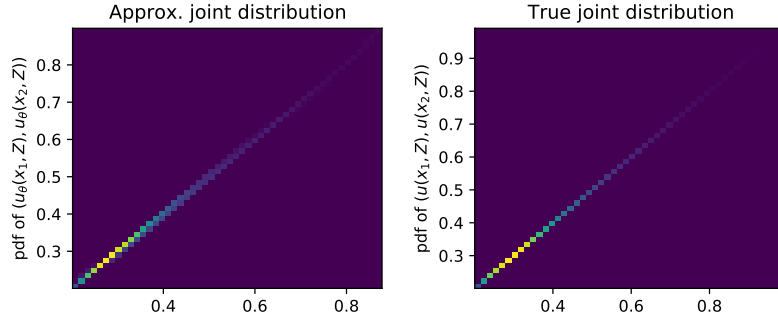


Figure 9: Joint distribution of the solution to the Dirichlet problem at $x_1 = (-0.5, -0.5)$ and $x_2 = (0.5, 0.5)$. Left: the approximated joint pdf of $u_\theta(x_1, Z)$ and $u_\theta(x_2, Z)$; Right: the exact joint pdf of $u(x_1, Z)$ and $u(x_2, Z)$.

4.4. Overdamped Langevin dynamics with Dirichlet boundary condition

As the final test problem, we consider the following d dimensional problem

$$\begin{aligned} -\nabla \cdot (\kappa(x, Z) \nabla u(x, Z)) &= f(x, Z) & \text{in } B(0, 1) \subset \mathbb{R}^d \\ u(x, Z) &= e^Z & \text{on } \partial B(0, 1), \end{aligned} \quad (14)$$

where the random field $\kappa(x, Z) = e^{-V(x, Z)}$ and $f(x, Z) = -d Z$ with

$$V(x, Z) = Z(1 + \|x\|^2)$$

and Z is uniform over $[-1/2, 1/2]$. The unique solution of the above problem is

$$u(x, Z) = e^{Z(1 + \|x\|^2)}.$$

Stochastic minimization of the loss function $J(\theta)$ associated with this problem involves uniform sampling in the ball $B(0,1)$, which can be performed by standard rejection sampling. However, for high dimensional problems (e.g., $d = 10$), the rejection sampling becomes infeasible due to the high rejection rate. We instead utilize the ball point picking algorithm to sample uniformly in $B(0,1)$ [47]. For the boundary penalty term this amounts to sampling a uniform random vector S on the sphere $\partial B(0,1) \in \mathbb{R}^d$. We use the fact that

$$S = \frac{(X_1, \dots, X_d)}{\sqrt{X_1^2 + \dots + X_d^2}}$$

is uniform on $\partial B(0,1)$ when X_1, \dots, X_d are independent identically distributed standard normal random variables.

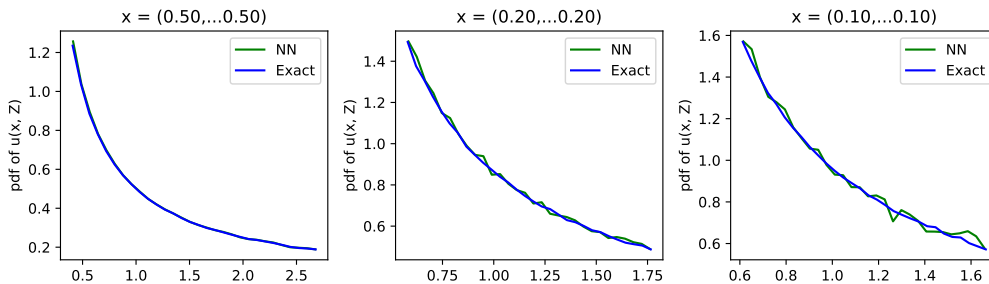


Figure 10: Marginal distributions of the solution to (14) with $d = 4$ and penalty coefficient $\beta = 500$. Left: the pdf of $u_\theta(x, Z)$ at $x = (0.5, \dots, 0.5) \in \mathbb{R}^4$; Center: the pdf of $u_\theta(x, Z)$ at $x = (0.2, \dots, 0.2) \in \mathbb{R}^4$; Right: the pdf of $u_\theta(x, Z)$ at $x = (0.1, \dots, 0.1) \in \mathbb{R}^4$.

The numerical experiments are carried out with $d = 4$ and $d = 10$. For both cases, we employ a 5-layer fully-connected DNN with $W = 256$ nodes per layer and we set mini-batch size to be 2560. The training of the DNN takes 3×10^5 epochs with an initial learning rate $\eta = 10^{-3}$ that is decreased by a factor of 10 after every 10^5 epochs. Finally, we choose the penalty coefficient $\lambda = 500$ to enforce the boundary condition. The numerical results for $d = 4$ and for $d = 10$ are presented in Figure 10 and Figure 11, respectively, displaying the distribution of the solution $u_\theta(x, Z)$ at different x . The relative L^2 mean errors are $E(\theta) = 0.19\%$ for $d = 4$ and $E(\theta) = 0.43\%$ for $d = 10$. The experiments, again, suggest that deep learning may overcome the curse of dimensionality exhibited by traditional discretization-based methods.

Summary and Conclusion

In this article, we have presented a stochastic deep-Ritz method for solving elliptic PDEs with random coefficients. The method employs the direct method of variational calculus to recast a random coefficient PDE into a stochastic minimization problem, which is subsequently solved by a combination of Monte Carlo sampling and DNN approximation.

Our method differs from traditional approaches for solving random coefficient PDEs in several key aspects. First and foremost, the utilization of the DNN approximation and

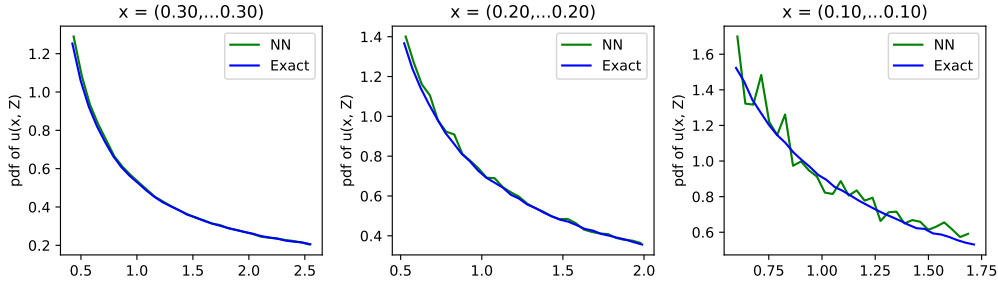


Figure 11: Marginal distributions of the solution to (14) with $d = 10$. Left: the pdf of $u_\theta(x, Z)$ at $x = (0.3, \dots, 0.3) \in \mathbb{R}^{10}$; Center: the pdf of $u_\theta(x, Z)$ at $x = (0.2, \dots, 0.2) \in \mathbb{R}^{10}$; Right: the pdf of $u_\theta(x, Z)$ at $x = (0.1, \dots, 0.1) \in \mathbb{R}^{10}$.

Monte Carlo sampling allows to avoid a discretization of the physical domain (e.g., finite element and finite volume) that often incurs an exponential growth of computational cost with the number of dimensions. Therefore, the method is applicable to problems with high dimensions in both physical space and stochastic space. Second, in comparison to the stochastic weak formulation, the stochastic variational formulation combined with DNN offers a natural loss function readily optimized by SGD methods. Moreover, the variational approach is well known to retain certain structures of the original problem and hence it is particularly advantageous when applied to structure preserving problems. Finally, unlike PINNs that require data points from the true solution, our method is “data free” as it relies only on a sampling over the input space in order to train the DNN.

Despite the above benefits, our method does suffer from several limitations. From the theoretical viewpoint, the lack of convergence result of our method makes the hyperparameter tuning ad-hoc. This issue becomes particularly challenging for high-dimensional problems. From the practical viewpoint, the boundary condition penalization incorporated in the loss function alters the ground truth and hence limits the superior accuracy of the method. Nevertheless, we comment that it is possible to transform a DNN to account for the boundary condition [48, 49]. Lastly, the Monte Carlo sampling over a general domain D can be quite challenging as it involves a constrained sampling over D and ∂D . For a complex domain D (e.g., with holes), the rejection sampling may become infeasible, especially in high dimension. In this case, an application of the constrained Markov chain Monte Carlo may be required [50, 51, 52, 53, 54].

Acknowledgments

The research of T.W. was sponsored by the DEVCOM Army Research Laboratory and was accomplished under Cooperative Agreement Number W911NF-16-2-0190. The views and conclusions contained in this document are those of the authors and should not be interpreted as representing the official policies, either expressed or implied, of the Army Research Laboratory or the U.S. Government. The U.S. Government is authorized to reproduce and distribute reprints for Government purposes notwithstanding any copyright notation herein.

References

- [1] I. Babuška, F. Nobile, R. Tempone, A stochastic collocation method for elliptic partial differential equations with random input data, *SIAM Journal on Numerical Analysis* 45 (3) (2007) 1005–1034.
- [2] F. Nobile, R. Tempone, C. G. Webster, A sparse grid stochastic collocation method for partial differential equations with random input data, *SIAM Journal on Numerical Analysis* 46 (5) (2008) 2309–2345.
- [3] F. Nobile, R. Tempone, C. G. Webster, An anisotropic sparse grid stochastic collocation method for partial differential equations with random input data, *SIAM Journal on Numerical Analysis* 46 (5) (2008) 2411–2442.
- [4] I. Babuska, R. Tempone, G. E. Zouraris, Galerkin finite element approximations of stochastic elliptic partial differential equations, *SIAM Journal on Numerical Analysis* 42 (2) (2004) 800–825.
- [5] H. G. Matthies, A. Keese, Galerkin methods for linear and nonlinear elliptic stochastic partial differential equations, *Computer methods in applied mechanics and engineering* 194 (12-16) (2005) 1295–1331.
- [6] F. Y. Kuo, D. Nuyens, Application of quasi-monte carlo methods to elliptic pdes with random diffusion coefficients: a survey of analysis and implementation, *Foundations of Computational Mathematics* 16 (6) (2016) 1631–1696.
- [7] R. G. Ghanem, P. D. Spanos, *Stochastic finite elements: a spectral approach*, Courier Corporation, 2003.
- [8] M. D. Gunzburger, C. G. Webster, G. Zhang, Stochastic finite element methods for partial differential equations with random input data, *Acta Numerica* 23 (2014) 521–650.
- [9] D. Xiu, G. E. Karniadakis, The Wiener–Askey polynomial chaos for stochastic differential equations, *SIAM journal on scientific computing* 24 (2) (2002) 619–644.
- [10] D. Xiu, G. E. Karniadakis, Modeling uncertainty in flow simulations via generalized polynomial chaos, *Journal of computational physics* 187 (1) (2003) 137–167.
- [11] P. Grohs, F. Hornung, A. Jentzen, P. Von Wurstemberger, A proof that artificial neural networks overcome the curse of dimensionality in the numerical approximation of black-scholes partial differential equations, *arXiv preprint arXiv:1809.02362* (2018).
- [12] T. Poggio, H. Mhaskar, L. Rosasco, B. Miranda, Q. Liao, Why and when can deep-but not shallow-networks avoid the curse of dimensionality: a review, *International Journal of Automation and Computing* 14 (5) (2017) 503–519.
- [13] M. Raissi, P. Perdikaris, G. E. Karniadakis, Physics-informed neural networks: A deep learning framework for solving forward and inverse problems involving nonlinear partial differential equations, *Journal of Computational physics* 378 (2019) 686–707.
- [14] M. Raissi, P. Perdikaris, G. E. Karniadakis, Physics informed deep learning (part i): Data-driven solutions of nonlinear partial differential equations, *arXiv preprint arXiv:1711.10561* (2017).
- [15] J. Sirignano, K. Spiliopoulos, Dgm: A deep learning algorithm for solving partial differential equations, *Journal of computational physics* 375 (2018) 1339–1364.
- [16] J. Berg, K. Nyström, A unified deep artificial neural network approach to partial differential equations in complex geometries, *Neurocomputing* 317 (2018) 28–41.
- [17] G. Carleo, M. Troyer, Solving the quantum many-body problem with artificial neural networks, *Science* 355 (6325) (2017) 602–606.
- [18] J. Han, A. Jentzen, et al., Deep learning-based numerical methods for high-dimensional parabolic partial differential equations and backward stochastic differential equations, *Communications in Mathematics and Statistics* 5 (4) (2017) 349–380.
- [19] J. Han, A. Jentzen, E. Weinan, Solving high-dimensional partial differential equations using deep learning, *Proceedings of the National Academy of Sciences* 115 (34) (2018) 8505–8510.
- [20] C. Beck, A. Jentzen, et al., Machine learning approximation algorithms for high-dimensional fully nonlinear partial differential equations and second-order backward stochastic differential equations, *Journal of Nonlinear Science* 29 (4) (2019) 1563–1619.
- [21] J. Han, et al., Deep learning approximation for stochastic control problems, *arXiv preprint arXiv:1611.07422* (2016).
- [22] N. Nüsken, L. Richter, Solving high-dimensional hamilton–jacobi–bellman pdes using neural networks: perspectives from the theory of controlled diffusions and measures on path space, *Partial Differential Equations and Applications* 2 (4) (2021) 1–48.
- [23] N. Nüsken, L. Richter, Interpolating between bsdes and pinns–deep learning for elliptic and parabolic boundary value problems, *arXiv preprint arXiv:2112.03749* (2021).

- [24] B. Yu, E. Weinan, The deep ritz method: a deep learning-based numerical algorithm for solving variational problems, *Communications in Mathematics and Statistics* 6 (1) (2018) 1–12.
- [25] Y. Khoo, J. Lu, L. Ying, Solving for high-dimensional committor functions using artificial neural networks, *Research in the Mathematical Sciences* 6 (1) (2019) 1–13.
- [26] Y. Khoo, J. Lu, L. Ying, Solving parametric pde problems with artificial neural networks, *European Journal of Applied Mathematics* 32 (3) (2021) 421–435.
- [27] J. Müller, M. Zeinhofer, Deep ritz revisited, arXiv preprint arXiv:1912.03937 (2019).
- [28] H. Li, L. Ying, A semigroup method for high dimensional elliptic pdes and eigenvalue problems based on neural networks, *Journal of Computational Physics* (2022) 110939.
- [29] C. Beck, M. Hutzenthaler, A. Jentzen, B. Kuckuck, An overview on deep learning-based approximation methods for partial differential equations, arXiv preprint arXiv:2012.12348 (2020).
- [30] E. Weinan, J. Han, A. Jentzen, Algorithms for solving high dimensional pdes: From nonlinear monte carlo to machine learning, *Nonlinearity* 35 (1) (2021) 278.
- [31] E. Weinan, Machine learning and computational mathematics, arXiv preprint arXiv:2009.14596 (2020).
- [32] Y. Zhu, N. Zabaras, P.-S. Koutsourelakis, P. Perdikaris, Physics-constrained deep learning for high-dimensional surrogate modeling and uncertainty quantification without labeled data, *Journal of Computational Physics* 394 (2019) 56–81.
- [33] X. Zhang, K. Garikipati, Bayesian neural networks for weak solution of pdes with uncertainty quantification, arXiv preprint arXiv:2101.04879 (2021).
- [34] L. Lu, P. Jin, G. E. Karniadakis, Deeponet: Learning nonlinear operators for identifying differential equations based on the universal approximation theorem of operators, arXiv preprint arXiv:1910.03193 (2019).
- [35] Z. Li, N. Kovachki, K. Azizzadenesheli, B. Liu, K. Bhattacharya, A. Stuart, A. Anandkumar, Fourier neural operator for parametric partial differential equations, arXiv preprint arXiv:2010.08895 (2020).
- [36] T. Wang, J. Knap, Stochastic gradient descent for semilinear elliptic equations with uncertainties, *Journal of Computational Physics* 426 (2021) 109945.
- [37] I. Goodfellow, J. Pouget-Abadie, M. Mirza, B. Xu, D. Warde-Farley, S. Ozair, A. Courville, Y. Bengio, Generative adversarial nets, *Advances in neural information processing systems* 27 (2014).
- [38] M. Arjovsky, S. Chintala, L. Bottou, Wasserstein generative adversarial networks, in: *International conference on machine learning*, PMLR, 2017, pp. 214–223.
- [39] Y. Zang, G. Bao, X. Ye, H. Zhou, Weak adversarial networks for high-dimensional partial differential equations, *Journal of Computational Physics* 411 (2020) 109409.
- [40] B. Dacorogna, *Direct methods in the calculus of variations*, Vol. 78, Springer Science & Business Media, 2007.
- [41] K. He, X. Zhang, S. Ren, J. Sun, Deep residual learning for image recognition, in: *Proceedings of the IEEE conference on computer vision and pattern recognition*, 2016, pp. 770–778.
- [42] S. Asmussen, P. W. Glynn, *Stochastic simulation: algorithms and analysis*, Vol. 57, Springer, 2007.
- [43] P. Glasserman, *Monte Carlo methods in financial engineering*, Vol. 53, Springer, 2004.
- [44] M. Struwe, *Variational methods*, Vol. 31999, Springer, 1990.
- [45] D. P. Kingma, J. Ba, Adam: A method for stochastic optimization, arXiv preprint arXiv:1412.6980 (2014).
- [46] A. Paszke, S. Gross, S. Chintala, G. Chanan, E. Yang, Z. DeVito, Z. Lin, A. Desmaison, L. Antiga, A. Lerer, *Automatic differentiation in pytorch* (2017).
- [47] F. Barthe, O. Guédon, S. Mendelson, A. Naor, A probabilistic approach to the geometry of the l_p^n -ball, *The Annals of Probability* 33 (2) (2005) 480–513.
- [48] J. Müller, M. Zeinhofer, Notes on exact boundary values in residual minimisation, arXiv preprint arXiv:2105.02550 (2021).
- [49] I. E. Lagaris, A. Likas, D. I. Fotiadis, Artificial neural networks for solving ordinary and partial differential equations, *IEEE transactions on neural networks* 9 (5) (1998) 987–1000.
- [50] W. Zhang, Ergodic sdes on submanifolds and related numerical sampling schemes, *ESAIM: Mathematical Modelling and Numerical Analysis* 54 (2) (2020) 391–430.
- [51] G. Ciccotti, T. Lelièvre, E. Vanden-Eijnden, Projection of diffusions on submanifolds: Application to mean force computation, *Communications on Pure and Applied Mathematics: A Journal Issued by the Courant Institute of Mathematical Sciences* 61 (3) (2008) 371–408.
- [52] T. Lelièvre, M. Rousset, G. Stoltz, Langevin dynamics with constraints and computation of free energy differences, *Mathematics of computation* 81 (280) (2012) 2071–2125.
- [53] E. Zappa, M. Holmes-Cerfon, J. Goodman, Monte carlo on manifolds: sampling densities and

- integrating functions, *Communications on Pure and Applied Mathematics* 71 (12) (2018) 2609–2647.
- [54] T. Lelièvre, M. Rousset, G. Stoltz, Hybrid monte carlo methods for sampling probability measures on submanifolds, *Numerische Mathematik* 143 (2) (2019) 379–421.